

XVII Marcel Grossmann Meeting - Pescara
Multi-Messenger parallel session, 12 July 2024

How to do multi-messenger forecasts in the Einstein Telescope era: addressing present and future challenges

Ulyana Dupletsa

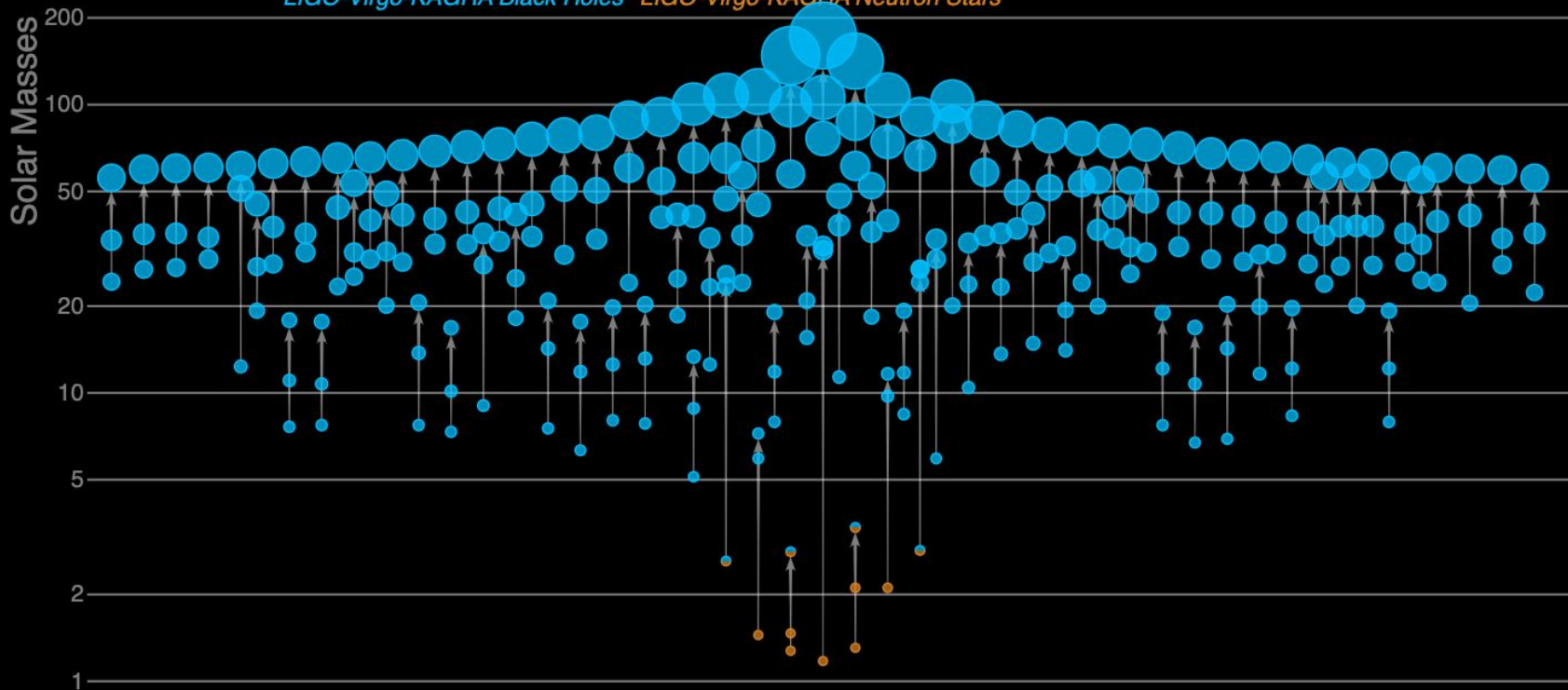
in collaboration with

Marica Branchesi, Biswajit Banerjee, Stefano Foffa, Jan Harms, Nandini Hazra,
Francesco Iacovelli, Eleonora Loffredo, Michele Mancarella, Michele Maggiore, Michela
Mapelli, Niccolò Muttoni, Samuele Ronchini, Filippo Santoliquido, Jacopo Tissino



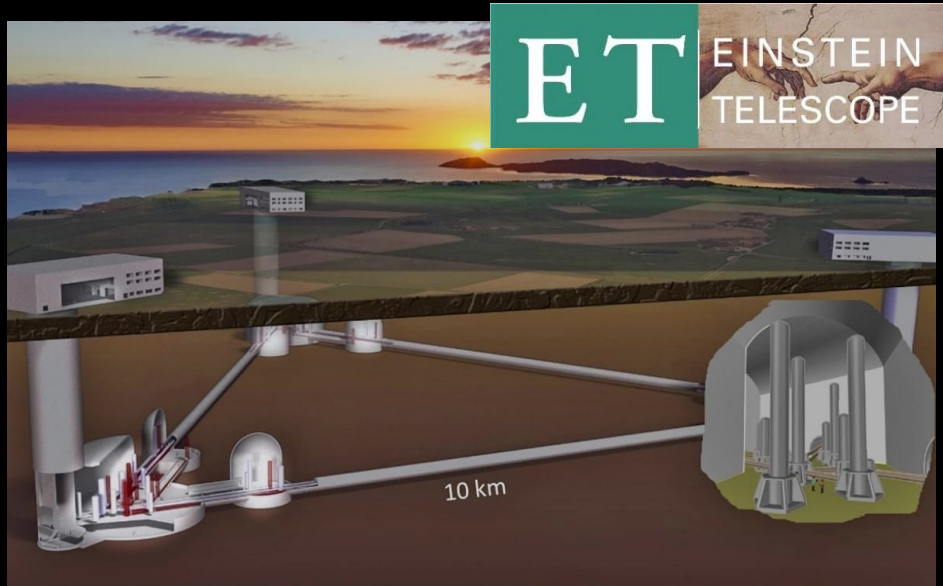
Masses in the Stellar Graveyard

LIGO-Virgo-KAGRA Black Holes *LIGO-Virgo-KAGRA Neutron Stars*

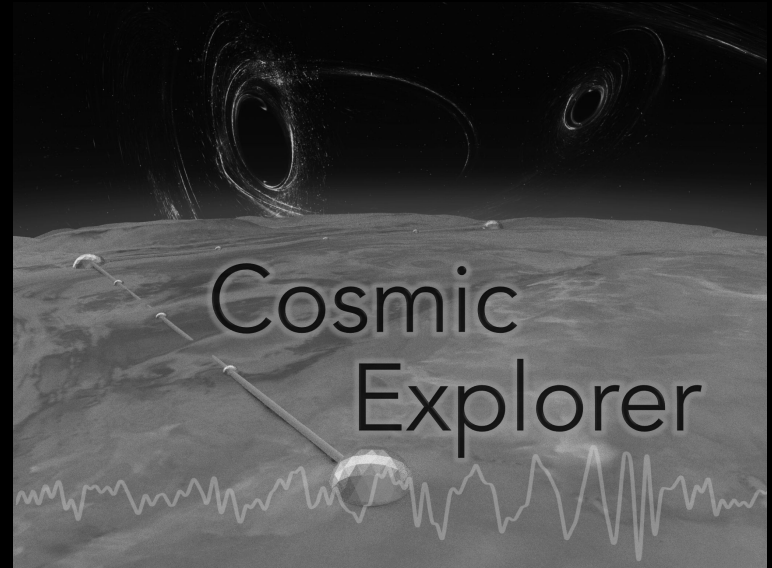
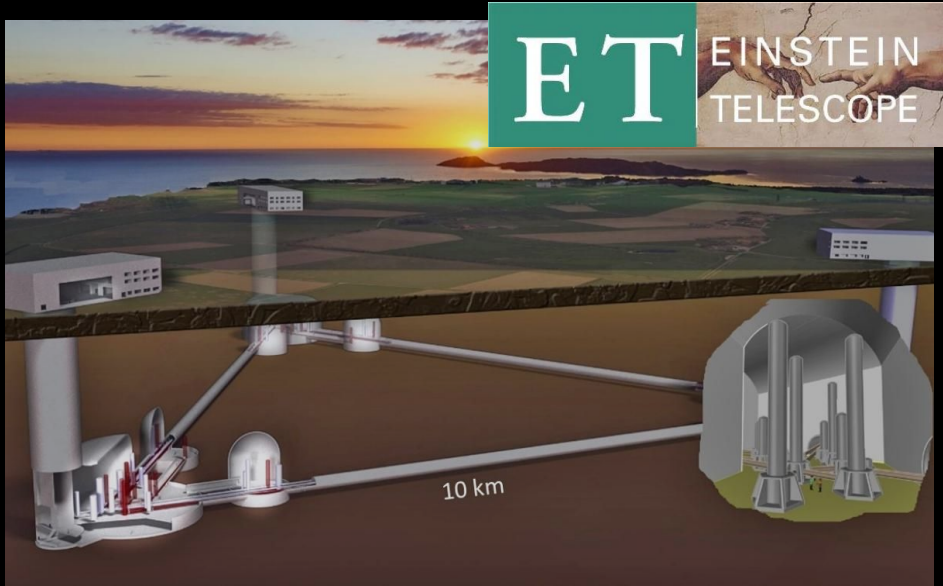


LIGO-Virgo-KAGRA | Aaron Geller | Northwestern

Next-generation ground-based GW detectors



Next-generation ground-based GW detectors



- $1e5$ BBHs
- $1e5$ BNSs

Science with the Einstein Telescope: a comparison of different designs

Marica Branchesi^{1,2,*}, Michele Maggiore^{3,4,*}, David Alonso⁵, Charles Badger⁶, Biswajit Banerjee^{1,2}, Freija Beirnaert⁷, Enis Belgacem^{3,4}, Swetna Bhatnagar^{8,9}, Guillaume Boileau^{10,11}, Ssohrab Borhanian¹², Daniel David Brown¹³, Man Leong Chan¹⁴, Giulia Cusin^{15,3,4}, Stefan L. Danilishin^{16,17}, Jerome Degallaix¹⁸, Valerio De Luca¹⁹, Arnab Dhani²⁰, Tim Dietrich^{21,22}, Ulyana Dupletsa^{1,2}, Stefano Foffa^{3,4}, Gabriele Franciolini⁸, Andreas Freise¹⁶, Gianluca Gemme², Boris Goncharov^{1,2}, Archisman Ghosh⁷, Francesca Gulminelli²³, Ish Gupta²⁴, Pawan Kumar Gupta^{16,2}, Jan Harms^{1,2}, Nandini Hazra^{1,2,27}, Stefan Hild^{16,17}, Tanja Hinderer²⁵, Ik Siang Heng²⁶, Francesco Iacovelli^{3,4}, Justin Janquart^{16,26}, Kamiel Janssens^{10,11}, Alexander C. Jenkins³⁰, Chinmay Kalaghatgi^{16,26,31}, Xhesika Korovesi^{32,33}, Tjonnie G.F. Li^{34,35}, Yufeng Li³⁶, Eleonora Loffredo^{1,2}, Elisa Maggio²², Michele Mancarella^{3,4,37,38}, Michela Mapelli^{39,40,41}, Katarina Martinovic⁴², Andrea Maselli^{1,2}, Patrick Meyers⁴², Andrew L. Miller^{43,16,26}, Chiranjib Mondal²⁹, Niccolò Muttoni^{3,4}, Harsh Narola^{16,26}, Micaela Oertel⁴⁴, Gor Oganessian¹, Costantino Pacilio^{8,37,38}, Cristiano Palomba⁴⁵, Paolo Pani³, Antonio Pasqualetti⁴⁶, Albino Perego^{47,48}, Carole PÉrigois^{39,40,41}, Mauro Pieroni^{49,50}, Ornella Juliana Piccinni⁵¹, Anna Puecher^{16,26}, Paola Punzo⁴⁵, Angelo Ricciardone^{52,39,40}, Antonio Riotto³, Samuele Ronchini^{1,2}, Mairi Sakellariadou⁶, Anuradha Samajdar²¹, Filippo Santoliquido^{39,40,41}, B.S. Sathyaprakash^{20,53,54}, Jessica Steinlechner^{16,17}, Sebastian Steinlechner^{16,17}, Andrei Utina^{16,17}, Chris Van Den Broeck^{16,26} and Teng Zhang^{9,17}

JCAP07 (2023) 068

Science Reference Paper for the CoBA study

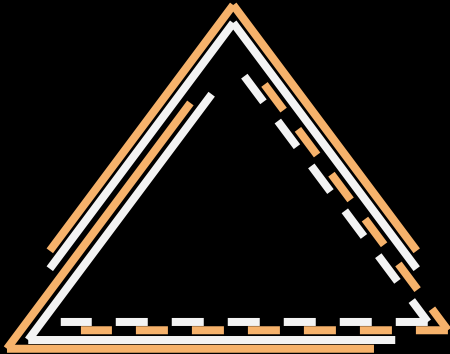
Work coordinated by Marica Branchesi and Michele Maggiore

(arXiv:2303.15923)

G S
S I

JCAP 07 (2023) 068

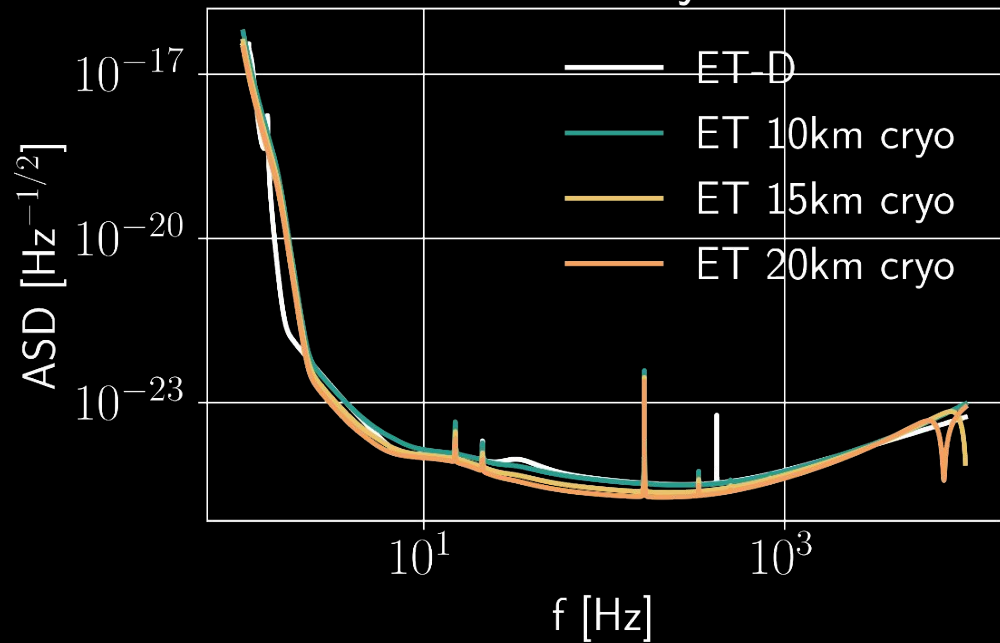
Reference Design of ET



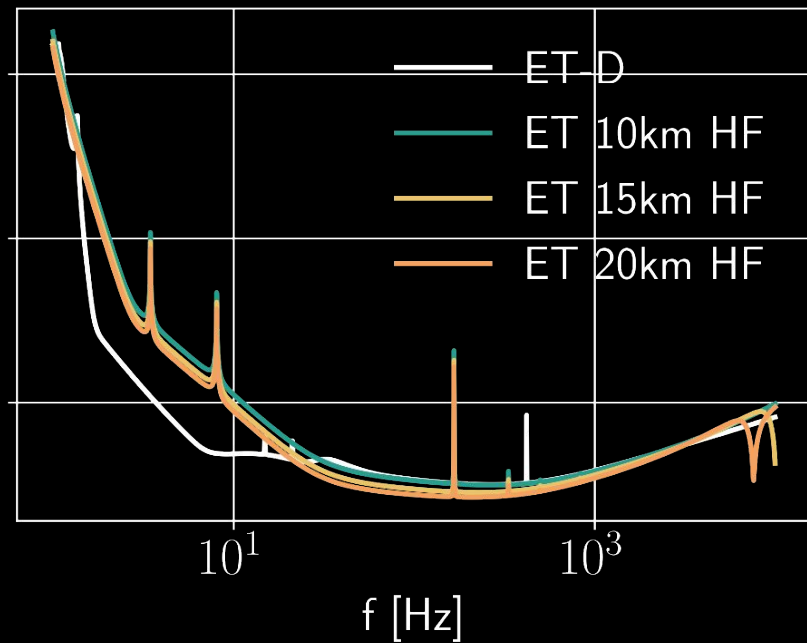
The reference ET configuration consists of:

- Triangular shape
- 10 km arms
- 3 nested detectors in xylophone configuration: HF + HFLF (cryogenic)

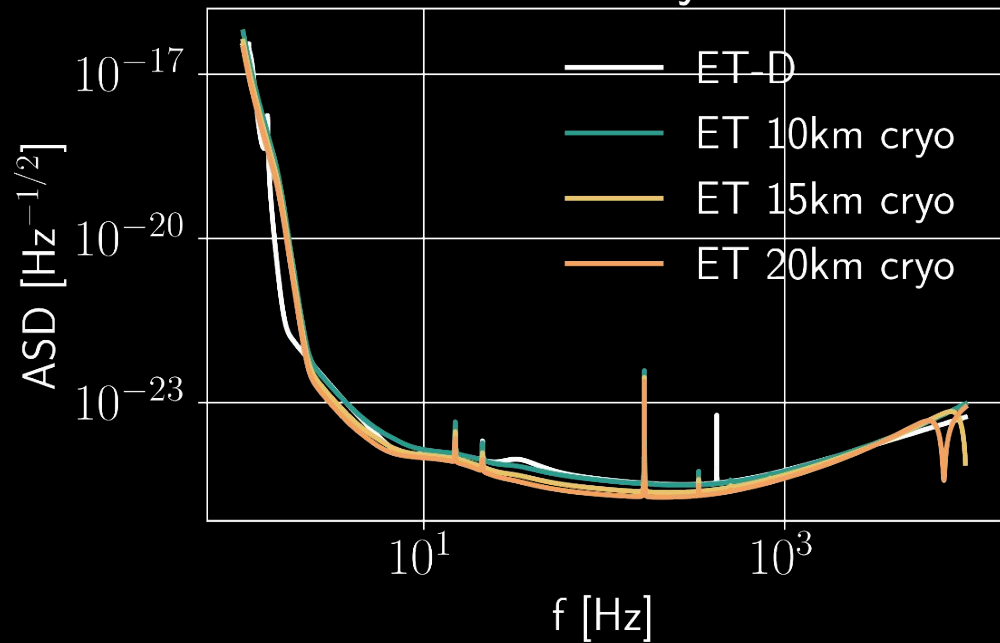
HFLF cryo



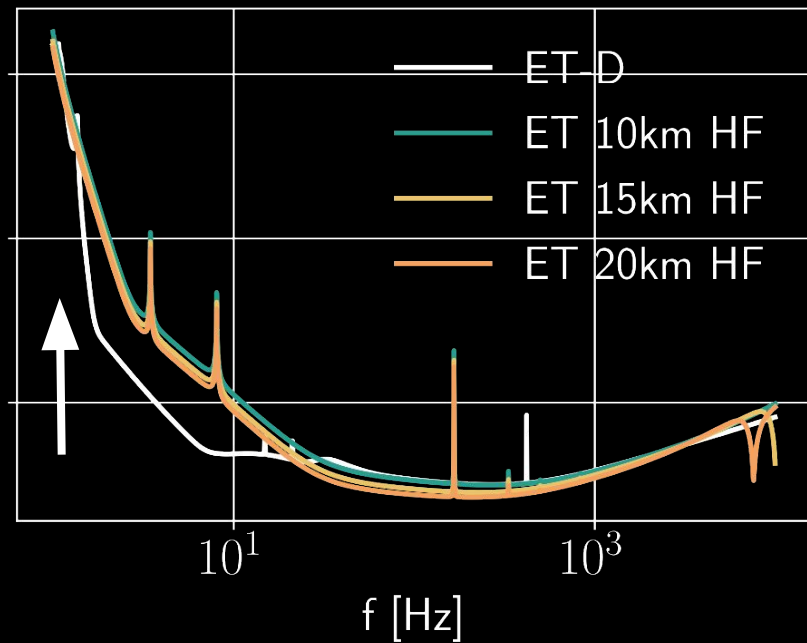
HF



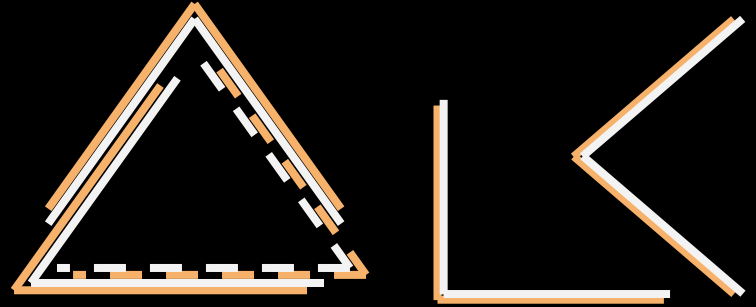
HFLF cryo



HF



Different Configurations



- Changes in geometry: triangle vs 2L, different arm lengths
- Role of the low frequency instrument: what happens if we have only the HF part?

- Triangle, 10 km arms
(reference design)
- 2L, 15 km arms, at 45°

- Triangle, 15 km arms
- 2L, 20 km arms, at 45°

From LVK parameter estimation to forecasts for ET

From signals to parameters

$$d = n + h(\vec{\theta}_{\text{true}})$$

From signals to parameters

$$d = n + h(\vec{\theta}_{\text{true}})$$

$$p(\vec{\theta}|d) \propto \mathcal{L}(\vec{\theta}|d)\pi(\vec{\theta})$$

From signals to parameters

$$d = n + h(\vec{\theta}_{\text{true}})$$

$$p(\vec{\theta}|d) \propto \mathcal{L}(\vec{\theta}|d)\pi(\vec{\theta})$$

$$\mathcal{L}(d|\vec{\theta}) \propto \exp \left[-\frac{1}{2} \langle d - h(\vec{\theta}) | d - h(\vec{\theta}) \rangle \right]$$

From signals to parameters

$$d = n + h(\vec{\theta}_{\text{true}})$$

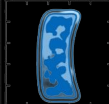
$$p(\vec{\theta}|d) \propto \mathcal{L}(\vec{\theta}|d)\pi(\vec{\theta})$$

$$\mathcal{L}(d|\vec{\theta}) \propto \exp \left[-\frac{1}{2} \langle d - h(\vec{\theta}) | d - h(\vec{\theta}) \rangle \right]$$

matched-filtering

takes into account the
sensitivity of the detector!

From signals to parameters



$$d = n + h(\vec{\theta}_{\text{true}})$$

$$p(\vec{\theta}|d) \propto \mathcal{L}(\vec{\theta}|d)\pi(\vec{\theta})$$

$$\mathcal{L}(d|\vec{\theta}) \propto \exp \left[-\frac{1}{2} \langle d - h(\vec{\theta}) | d - h(\vec{\theta}) \rangle \right]$$

matched-filtering

takes into account the
sensitivity of the detector!

Forecasts for 3G Detectors


- Fisher matrix codes are **particularly useful to study the performance of future GW observatories**
- **Computationally convenient:** we can easily study entire populations ($\sim 1e5$ events): each event takes fraction of a second to complete, which is to compare with full PE softwares as **Bilby** that take order of days to process a GW event

Fisher Matrix Primer

$$\mathcal{L}(d|\vec{\theta}) \propto \exp \left[-\frac{1}{2} \langle d - h(\vec{\theta}) | d - h(\vec{\theta}) \rangle \right]$$

$$h(\vec{\theta}) = h_0 + \Delta\theta^i h_i$$

expand around the true
value at first order

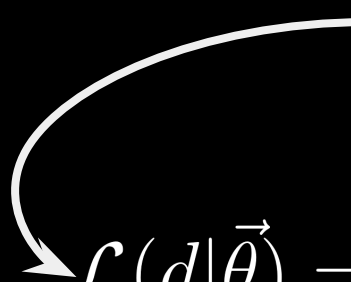

$$\mathcal{L}(d|\vec{\theta}) = \exp \left[-\frac{1}{2} \Delta\theta^i \langle h_i | h_j \rangle \Delta\theta^j \right]$$

Fisher Matrix Primer

$$\mathcal{L}(d|\vec{\theta}) \propto \exp \left[-\frac{1}{2} \langle d - h(\vec{\theta}) | d - h(\vec{\theta}) \rangle \right]$$

$$h(\vec{\theta}) = h_0 + \Delta\theta^i h_i$$

expand around the true
value at first order


$$\mathcal{L}(d|\vec{\theta}) = \exp \left[-\frac{1}{2} \Delta\theta^i \langle h_i | h_j \rangle \Delta\theta^j \right]$$

**Gaussian
Likelihood**

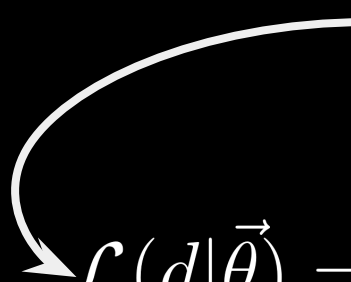
Fisher Matrix

Fisher Matrix Primer

$$\mathcal{L}(d|\vec{\theta}) \propto \exp \left[-\frac{1}{2} \langle d - h(\vec{\theta}) | d - h(\vec{\theta}) \rangle \right]$$

$$h(\vec{\theta}) = h_0 + \Delta\theta^i h_i$$

expand around the true
value at first order


$$\mathcal{L}(d|\vec{\theta}) = \exp \left[-\frac{1}{2} \Delta\theta^i \langle h_i | h_j \rangle \Delta\theta^j \right]$$

**Gaussian
Likelihood**

Fisher Matrix

$$\Delta\theta^i = \theta^i - \theta_{inj}^i$$

gwbench

S. Borhanian,
2021

[GitLab link](#)

GWFAST

F. Iacovelli,
M. Mancarella, et
al.
2022

[GitHub link](#)

TiDoFM

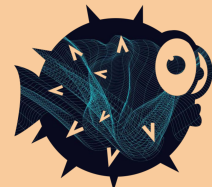
Li et al.
2022

[GitHub link](#)

GWFish

U. Dupletsa, J. Harms,
et al.
2022

[GitHub link](#)



GW FISH

gwbench

S. Borhanian,
2021

[GitLab link](#)

GWFAST

F. Iacovelli,
M. Mancarella, et
al.
2022

[GitHub link](#)

TiDoFM

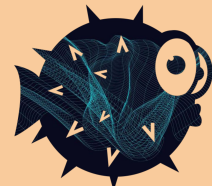
Li et al.
2022

[GitHub link](#)

GWFish

U. Dupletsa, J. Harms,
et al.
2022

[GitHub link](#)



GW FISH

Science with the Einstein Telescope: a comparison of different designs

Marica Branchesi^{1,2,*}, Michele Maggiore^{3,4,*}, David Alonso,⁵
Charles Badger,⁶ Biswajit Banerjee,^{1,2} Freija Beirnaert,⁷
Enis Belgacem,^{3,4} Swetna Bhatnagar,^{8,9} Guillaume Boileau,^{10,11}
Ssohrab Borhanian,¹² Daniel David Brown,¹³ Man Leong Chan,¹⁴
Giulia Cusin,^{15,3,4} Stefan L. Danilishin,^{16,17} Jerome Degallaix,¹⁸
Valerio De Luca,¹⁹ Arnab Dhani,²⁰ Tim Dietrich,^{21,22}
Ulyana Dupletsa,^{1,2} Stefano Foffa,^{3,4} Gabriele Franciolini,⁸
Andreas Freise,¹⁶ Gianluca Gemme,² Boris Goncharov,²
Archisman Ghosh,⁷ Francesca Gulminelli,²³ Ish Gupta,²⁴
Pawan Kumar Gupta,^{16,2} Jan Harms,^{1,2} Nandini Hazra,^{1,2,27}
Stefan Hild,^{16,17} Tanja Hinderer,²⁵ IK Siang Heng,²⁶
Francesco Iacovelli,^{3,4} Justin Janquart,^{16,26} Kamiel Janssens,^{10,11}
Alexander C. Jenkins,³⁰ Chinmay Kalaghatgi,^{16,26,31}
Xhesika Korovesi,^{32,33} Tjonnie G.F. Li,^{34,35} Yufeng Li,³⁶
Eleonora Loffredo,^{1,2} Elisa Maggio,²² Michele Mancarella,^{3,4,37,38}
Michela Mapelli,^{39,40,41} Katarina Martinovic,⁴² Andrea Maselli,^{1,2}
Patrick Meyers,⁴² Andrew L. Miller,^{43,16,26} Chiranjib Mondal,²⁹
Niccolò Muttoni,^{3,4} Harsh Narola,^{16,26} Micaela Oertel,⁴⁴
Gor Oganessian,¹ Costantino Pacilio,^{8,37,38} Cristiano Palomba,⁴⁵
Paolo Pani,³ Antonio Pasqualetti,⁴⁶ Albino Perego,^{47,48}
Carole PÉrigois,^{39,40,41} Mauro Pieroni,^{49,50}
Ornella Juliana Piccinni,⁵¹ Anna Puecher,^{16,26} Paola Punzo,⁴⁵
Angelo Ricciardone,^{52,39,40} Antonio Riotto,³ Samuele Ronchini,^{1,2}
Mairi Sakellariadou,⁶ Anuradha Samajdar,²¹
Filippo Santoliquido,^{39,40,41} B.S. Sathyaprakash,^{20,53,54}
Jessica Steinlechner,^{16,17} Sebastian Steinlechner,^{16,17}
Andrei Utina,^{16,17} Chris Van Den Broeck,^{16,26} and Teng Zhang^{9,17}

JCAP07 (2023) 068

Science Reference Paper for the CoBA study

Work coordinated by
Marica Branchesi and
Michele Maggiore

(arXiv:2303.15923)

G S
S I

JCAP 07 (2023) 068

Contents

1. **Introduction**
2. **Detector geometries and sensitivity curves**
3. **Coalescence of compact binaries**
 - 3.1. **Binary Black Hole**
 - 3.1.1. Comparison between geometries
 - 3.1.2. Effects of a change in the ASD
 - 3.1.3. Golden events
 - 3.2. **Binary Neutron Stars**
 - 3.2.1. Comparison between geometries
 - 3.2.2. Effects of a change in the ASD
 - 3.2.3. Golden events
 - 3.2.4. Dependence on the population model
 - 3.3. **ET in a network of 3G detectors**
4. **Multi-messenger astrophysics**
 - 4.1. **BNS sky-localization and pre-merger alerts**
 - 4.2. **Gamma-ray bursts: joint GW and high-energy detections**
 - 4.2.1. Prompt emission
 - 4.2.2. Afterglow: survey and pointing modes
 - 4.3. **Kilonovae: joint GW and optical detections**
5. **Stochastic backgrounds**
 - 5.1. **Sensitivity to isotropic stochastic backgrounds**
 - 5.2. **Angular sensitivity**
 - 5.3. **Astrophysical backgrounds**
 - 5.4. **Impact of correlated magnetic, seismic and Newtonian noise**
 - 5.4.1. Seismic and Newtonian Noise
 - 5.4.2. Magnetic noise
6. **Impacts of detector designs on specific science case**
 - 6.1. **Physics near the BH horizon**
 - 6.1.1. Testing the GR predictions for space-time dynamics near the horizon
 - 6.1.2. Searching for echoes and near-horizon structures
 - 6.1.3. Constraining tidal effects and multipolar structure
 - 6.2. **Nuclear physics**
 - 6.2.1. Radius estimation from Fisher-matrix computation
 - 6.2.2. Full parameter estimation results
 - 6.2.3. Connected uncertainty of nuclear-physics parameters
 - 6.2.4. Postmerger detectability
 - 6.2.5. Conclusions: nuclear physics with ET
 - 6.3. **Population studies**
 - 6.3.1. Merger rate reconstruction
 - 6.3.2. Constraints on PBHS from high-redshift mergers
 - 6.3.3. Other PBH signatures
 - 6.4. **Cosmology**
 - 6.4.1. Hubble parameter and dark energy from joint GW/EM detections
 - 6.4.2. Hubble parameter and dark energy from BNS tidal deformability
 - 6.4.3. Hubble parameter from high-mass ratio events
 - 6.5. **Cosmological stochastic backgrounds**
 - 6.5.1. Cosmic Strings
 - 6.5.2. First-order phase transition
 - 6.5.3. Source separation
 - 6.6. **Continuous waves**
 - 6.6.1. CWs from spinning neutron stars
 - 6.6.2. Transient CWs
 - 6.6.3. Search for dark matter with CWs
 - 6.7. **Conclusions**
7. **The role of the null stream in the triangle-2L comparison**

Contents

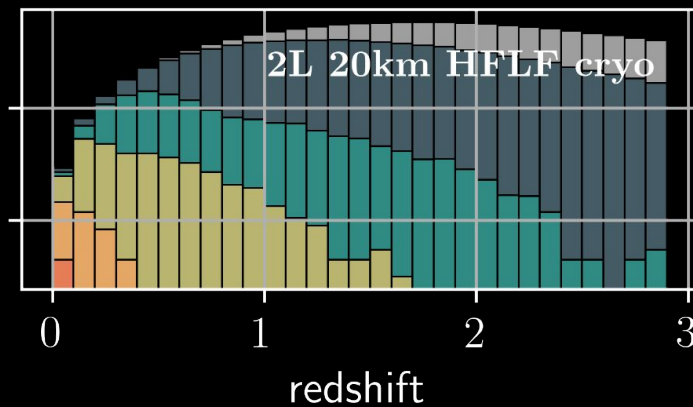
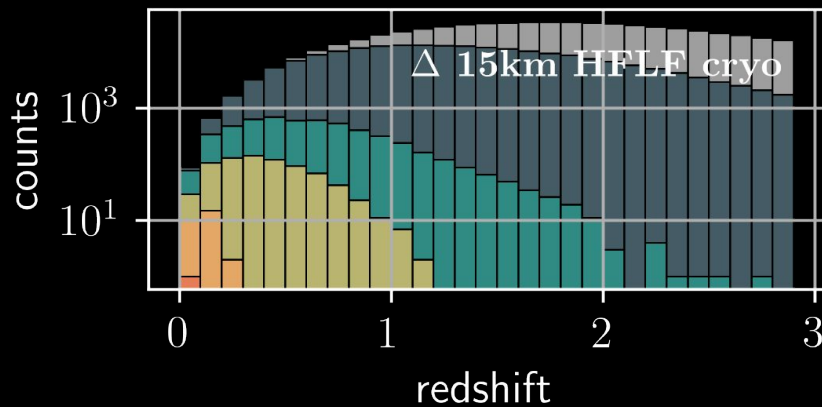
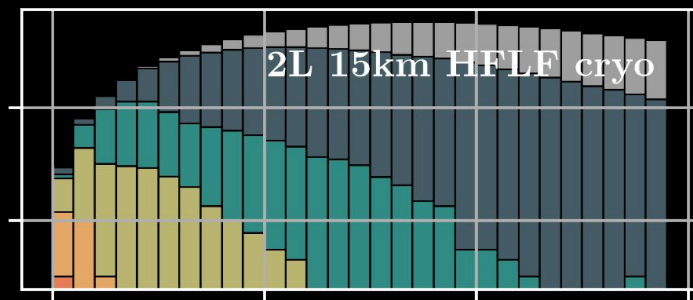
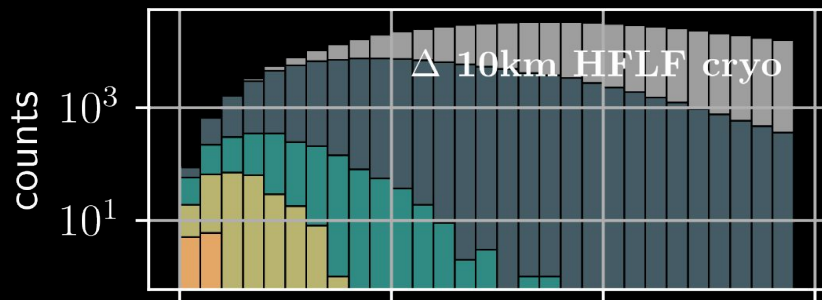
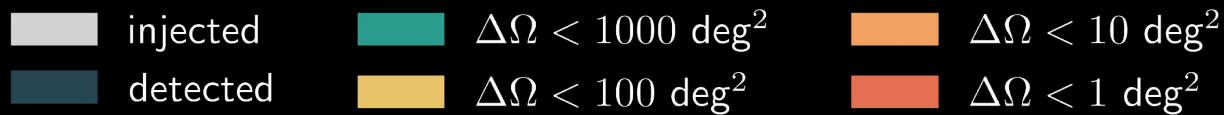
1. **Introduction**
2. **Detector geometries and sensitivity curves**
3. **Coalescence of compact binaries**
 - 3.1. **Binary Black Hole**
 - 3.1.1. Comparison between geometries
 - 3.1.2. Effects of a change in the ASD
 - 3.1.3. Golden events
 - 3.2. **Binary Neutron Stars**
 - 3.2.1. Comparison between geometries
 - 3.2.2. Effects of a change in the ASD
 - 3.2.3. Golden events
 - 3.2.4. Dependence on the population model
 - 3.3. **ET in a network of 3G detectors**
4. **Multi-messenger astrophysics**
 - 4.1. **BNS sky-localization and pre-merger alerts**
 - 4.2. **Gamma-ray bursts: joint GW and high-energy detections**
 - 4.2.1. **Prompt emission**
 - 4.2.2. **Afterglow: survey and pointing modes**
 - 4.3. **Kilonovae: joint GW and optical detections**
5. **Stochastic backgrounds**
 - 5.1. **Sensitivity to isotropic stochastic backgrounds**
 - 5.2. **Angular sensitivity**
 - 5.3. **Astrophysical backgrounds**
 - 5.4. **Impact of correlated magnetic, seismic and Newtonian noise**
 - 5.4.1. Seismic and Newtonian Noise
 - 5.4.2. Magnetic noise
6. **Impacts of detector designs on specific science case**
 - 6.1. **Physics near the BH horizon**
 - 1.1.1. Testing the GR predictions for space-time dynamics near the horizon
 - 1.1.2. Searching for echoes and near-horizon structures
 - 1.1.3. Constraining tidal effects and multipolar structure
7. **The role of the null stream in the triangle-2L comparison**
 - 1.2. **Nuclear physics**
 - 1.2.1. Radius estimation from Fisher-matrix computation
 - 1.2.2. Full parameter estimation results
 - 1.2.3. Connected uncertainty of nuclear-physics parameters
 - 1.2.4. Postmerger detectability
 - 1.2.5. Conclusions: nuclear physics with ET
 - 1.3. **Population studies**
 - 1.3.1. Merger rate reconstruction
 - 1.3.2. Constraints on PBHS from high-redshift mergers
 - 1.3.3. Other PBH signatures
 - 1.4. **Cosmology**
 - 1.4.1. Hubble parameter and dark energy from joint GW/EM detections
 - 1.4.2. Hubble parameter and dark energy from BNS tidal deformability
 - 1.4.3. Hubble parameter from high-mass ratio events
 - 1.5. **Cosmological stochastic backgrounds**
 - 1.5.1. Cosmic Strings
 - 1.5.2. First-order phase transition
 - 1.5.3. Source separation
 - 1.6. **Continuous waves**
 - 1.6.1. CWs from spinning neutron stars
 - 1.6.2. Transient CWs
 - 1.6.3. Search for dark matter with CWs
 - 1.7. **Conclusions**

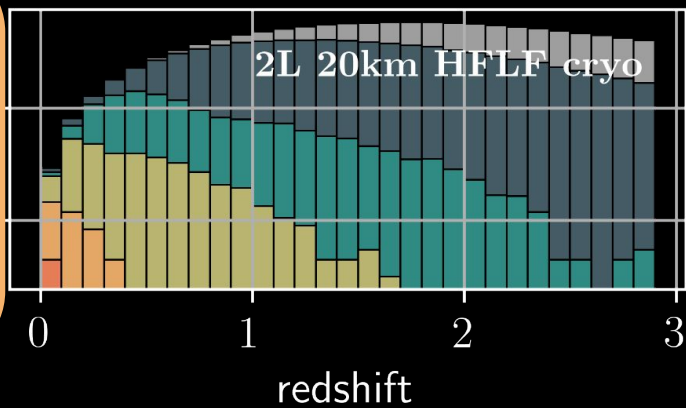
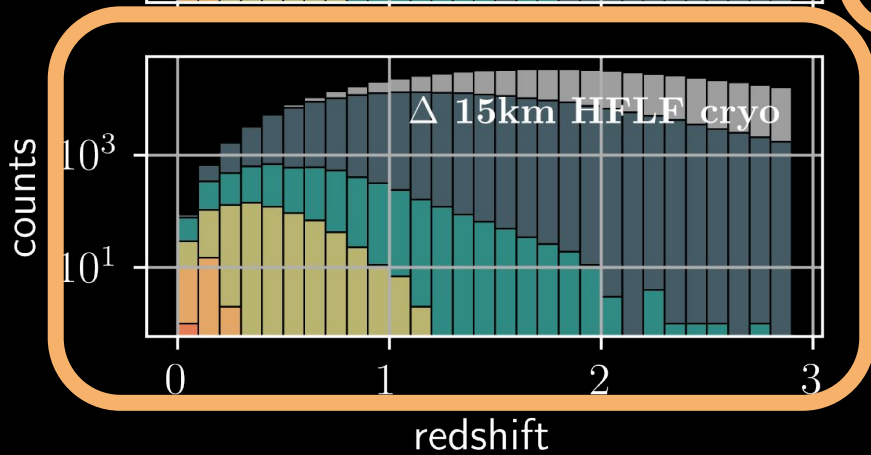
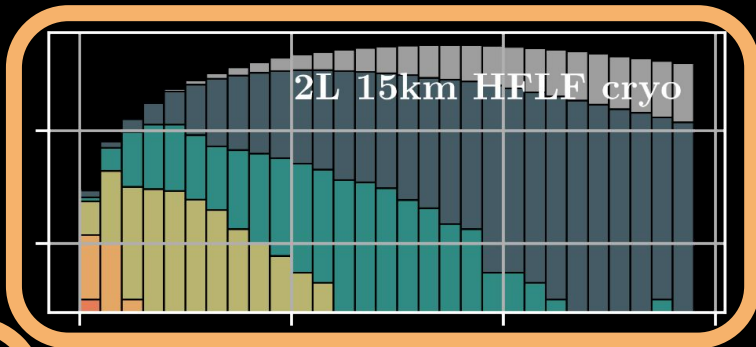
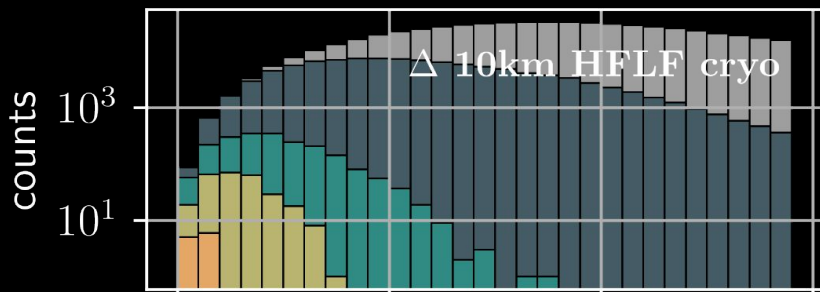
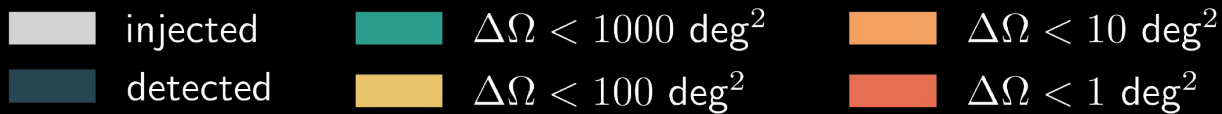
Starting Assumptions

- **IMRPhenomD_NRTidalv2**
- The BNS population was obtained using **MOBSE** (isolated binaries) with a local merger rate of $250 \text{ Gpc}^{-3} \text{ yr}^{-1}$ (to compare to the LVK result of 10-1700 $\text{Gpc}^{-3} \text{ yr}^{-1}$)
- 1 year of observations

Multi-Messenger Astronomy

Sky Localization





Full (HFLF cryo) sensitivity detectors

$\Delta\Omega_{90\%}$ [deg ²]	All orientation BNSs				BNSs with $\Theta_v < 15^\circ$			
	$\Delta 10$	$\Delta 15$	2L 15	2L 20	$\Delta 10$	$\Delta 15$	2L 15	2L 20
10	11	27	24	45	0	1	2	5
40	78	215	162	350	8	22	20	33
100	280	764	644	1282	26	74	68	133
10000	2112	5441	7478	13482	272	632	1045	1725

Full (HFLF cryo) sensitivity detectors

$\Delta\Omega_{90\%}$ [deg ²]	All orientation BNSs				BNSs with $\Theta_v < 15^\circ$			
	$\Delta 10$	$\Delta 15$	2L 15	2L 20	$\Delta 10$	$\Delta 15$	2L 15	2L 20
10	11	27	24	45	0	1	2	5
40	78	215	162	350	8	22	20	33
100	280	764	644	1282	26	74	68	133
10000	2112	5441	7478	13482	272	632	1045	1725

Full (HFLF cryo) sensitivity detectors

$\Delta\Omega_{90\%}$ [deg ²]	All orientation BNSs				BNSs with $\Theta_v < 15^\circ$			
	$\Delta 10$	$\Delta 15$	2L 15	2L 20	$\Delta 10$	$\Delta 15$	2L 15	2L 20
10	11	27	24	45	0	1	2	5
40	78	215	162	350	8	22	20	33
100	280	764	644	1282	26	74	68	133
10000	2112	5441	7478	13482	272	632	1045	1725

HF sensitivity detectors

$\Delta\Omega_{90\%}$ [deg ²]	All orientation BNSs				BNSs with $\Theta_v < 15^\circ$			
	$\Delta 10$	$\Delta 15$	2L 15	2L 20	$\Delta 10$	$\Delta 15$	2L 15	2L 20
10	0	1	5	5	0	0	2	2
40	4	10	20	47	0	5	6	17
100	14	53	76	144	7	33	35	64
10000	145	548	1662	3378	80	336	672	1302

Full (HFLF cryo) sensitivity detectors								
$\Delta\Omega_{90\%}$ [deg ²]	All orientation BNSs				BNSs with $\Theta_v < 15^\circ$			
	$\Delta 10$	$\Delta 15$	2L 15	2L 20	$\Delta 10$	$\Delta 15$	2L 15	2L 20
10	11	27	24	45	0	1	2	5
40	78	215	162	350	8	22	20	33
100	280	764	644	1282	26	74	68	133
10000	2112	5441	7478	13482	272	632	1045	1725

HF sensitivity detectors								
$\Delta\Omega_{90\%}$ [deg ²]	All orientation BNSs				BNSs with $\Theta_v < 15^\circ$			
	$\Delta 10$	$\Delta 15$	2L 15	2L 20	$\Delta 10$	$\Delta 15$	2L 15	2L 20
10	0	1	5	5	0	0	2	2
40	4	10	20	47	0	5	6	17
100	14	53	76	144	7	33	35	64
10000	145	548	1662	3378	80	336	672	1302

Full (HFLF cryo) sensitivity detectors								
$\Delta\Omega_{90\%}$ [deg ²]	All orientation BNSs				BNSs with $\Theta_v < 15^\circ$			
	$\Delta 10$	$\Delta 15$	2L 15	2L 20	$\Delta 10$	$\Delta 15$	2L 15	2L 20
10	11	27	24	45	0	1	2	5
40	78	215	162	350	8	22	20	33
100	280	764	644	1282	26	74	68	133
10000	2112	5441	7478	13482	272	632	1045	1725

HF sensitivity detectors								
$\Delta\Omega_{90\%}$ [deg ²]	All orientation BNSs				BNSs with $\Theta_v < 15^\circ$			
	$\Delta 10$	$\Delta 15$	2L 15	2L 20	$\Delta 10$	$\Delta 15$	2L 15	2L 20
10	0	1	5	5	0	0	2	2
40	4	10	20	47	0	5	6	17
100	14	53	76	144	7	33	35	64
10000	145	548	1662	3378	80	336	672	1302

Full (HFLF cryo) sensitivity detectors								
$\Delta\Omega_{90\%}$ [deg ²]	All orientation BNSs				BNSs with $\Theta_v < 15^\circ$			
	$\Delta 10$	$\Delta 15$	2L 15	2L 20	$\Delta 10$	$\Delta 15$	2L 15	2L 20
10	11	27	24	45	0	1	2	5
40	78	215	162	350	8	22	20	33
100	280	764	644	1282	26	74	68	133
10000	2112	5441	7478	13482	272	632	1045	1725

HF sensitivity detectors								
$\Delta\Omega_{90\%}$ [deg ²]	All orientation BNSs				BNSs with $\Theta_v < 15^\circ$			
	$\Delta 10$	$\Delta 15$	2L 15	2L 20	$\Delta 10$	$\Delta 15$	2L 15	2L 20
10	0	1	5	5	0	0	2	2
40	4	10	20	47	0	5	6	17
100	14	53	76	144	7	33	35	64
10000	145	548	1662	3378	80	336	672	1302

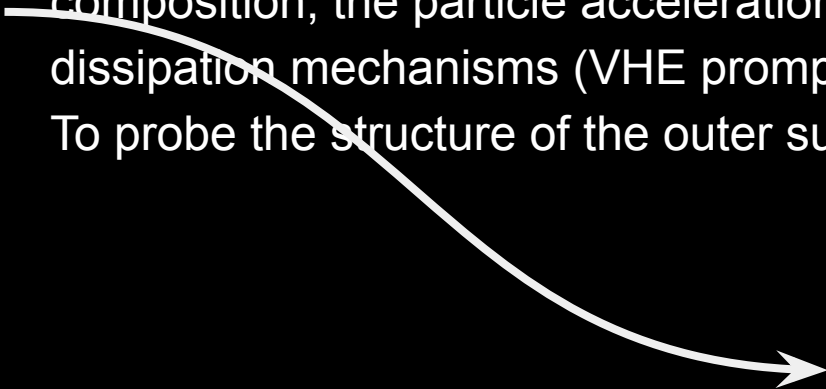
Pre-Merger Alerts

detections within $z < 1.5$

The importance of pre-merger alerts

Pre-merger detections are critical to detect the prompt/early multi-wavelength emission in order to:

- Probe the central engine of GRBs, and in particular to understand the jet composition, the particle acceleration mechanism, the radiation and energy dissipation mechanisms (VHE prompt CTA/ET synergy)
- To probe the structure of the outer sub-relativistic ejecta, early UV emission



[**B. Banerjee** et al.,
Astronomy&Astrophysics 678
(2023) A126]

Full (HFLF) cryo sensitivity detectors

Configuration	$\Delta\Omega_{90\%}$	All orientation BNSs			BNSs with $\Theta_v < 15^\circ$		
	[deg ²]	30 min	10 min	1 min	30 min	10 min	1 min
$\Delta 10$ km	10	0	1	5	0	0	0
	100	10	39	113	2	8	20
	1000	85	293	819	10	34	132
	All detected	905	4343	23597	81	393	2312
$\Delta 15$ km	10	1	5	11	0	1	1
	100	41	109	281	6	14	36
	1000	279	806	2007	33	102	295
	All detected	2489	11303	48127	221	1009	4024
2L 15 km	10	0	1	8	0	0	0
	100	20	54	169	2	7	26
	1000	194	565	1399	23	73	199
	All detected	2172	9598	39499	198	863	3432
2L 20 km	10	2	4	15	1	1	2
	100	39	118	288	7	19	47
	1000	403	1040	2427	47	128	346
	All detected	4125	17294	56611	363	1588	4377

Full (HFLF) cryo sensitivity detectors

Configuration	$\Delta\Omega_{90\%}$	All orientation BNSs			BNSs with $\Theta_v < 15^\circ$		
	[deg ²]	30 min	10 min	1 min	30 min	10 min	1 min
$\Delta 10$ km	10	0	1	5	0	0	0
	100	10	39	113	2	8	20
	1000	85	293	819	10	34	132
	All detected	905	4343	23597	81	393	2312
$\Delta 15$ km	10	1	5	11	0	1	1
	100	41	109	281	6	14	36
	1000	279	806	2007	33	102	295
	All detected	2489	11303	48127	221	1009	4024
2L 15 km	10	0	1	8	0	0	0
	100	20	54	169	2	7	26
	1000	194	565	1399	23	73	199
	All detected	2172	9598	39499	198	863	3432
2L 20 km	10	2	4	15	1	1	2
	100	39	118	288	7	19	47
	1000	403	1040	2427	47	128	346
	All detected	4125	17294	56611	363	1588	4377

HF sensitivity detectors

Configuration	$\Delta\Omega_{90\%}$	All orientation BNSs			BNSs with $\Theta_v < 15^\circ$		
	[deg ²]	30 min	10 min	1 min	30 min	10 min	1 min
$\Delta 10$ km	100	0	0	0	0	0	0
	1000	0	0	4	0	0	1
	All detected	0	3	317	0	0	26
$\Delta 15$ km	100	0	0	2	0	0	0
	1000	0	0	10	0	0	4
	All detected	2	8	891	0	1	84
2L 15 km	100	0	0	0	0	0	0
	1000	0	0	7	0	0	3
	All detected	0	7	743	0	1	69
2L 20 km	100	0	0	3	0	0	0
	1000	0	0	13	0	0	6
	All detected	2	11	1535	0	1	146

HF sensitivity detectors

Configuration	$\Delta\Omega_{90\%}$	All orientation BNSs			BNSs with $\Theta_v < 15^\circ$		
	[deg ²]	30 min	10 min	1 min	30 min	10 min	1 min
$\Delta 10$ km	100	0	0	0	0	0	0
	1000	0	0	4	0	0	1
	All detected	0	3	317	0	0	26
$\Delta 15$ km	100	0	0	2	0	0	0
	1000	0	0	10	0	0	4
	All detected	2	8	891	0	1	84
2L 15 km	100	0	0	0	0	0	0
	1000	0	0	7	0	0	3
	All detected	0	7	743	0	1	69
2L 20 km	100	0	0	3	0	0	0
	1000	0	0	13	0	0	6
	All detected	2	11	1535	0	1	146

HF sensitivity detectors							
Configuration	$\Delta\Omega_{90\%}$	All orientation BNSs			BNSs with $\Theta_v < 15^\circ$		
	[deg ²]	30 min	10 min	1 min	30 min	10 min	1 min
$\Delta 10$ km	100	0	0	0	0	0	0
	1000	0	0	4	0	0	1
	All detected	0	3	317	0	0	26
$\Delta 15$ km	100	0	0	2	0	0	0
	1000	0	0	10	0	0	4
	All detected	2	8	891	0	1	84
2L 15 km	100	0	0	0	0	0	0
	1000	0	0	7	0	0	3
	All detected	0	7	743	0	1	69
2L 20 km	100	0	0	3	0	0	0
	1000	0	0	13	0	0	6
	All detected	2	11	1535	0	1	146

No localized pre-merger detections!

Applications to Cosmology

Cosmology: ET + VRO

See Eleonora's talk!

- Joint GW-kilonova detections!
- 1 year of observations
- 115 joint detections for 2L-20km-cryo
- Dependence on BNS merger rate normalization



Cosmology: ET + VRO

HFLF cryogenic		
Configuration	$\Delta H_0/H_0$	$\Delta \Omega_M/\Omega_M$
$\Delta 10$ km	0.009	0.832
$\Delta 15$ km	0.007	0.303
2L 15 km	0.006	0.370
2L 20 km	0.004	0.243

HF only		
Configuration	$\Delta H_0/H_0$	$\Delta \Omega_M/\Omega_M$
$\Delta 10$ km	0.065	1.23
$\Delta 15$ km	0.057	1.86
2L 15 km	0.066	1.31
2L 20 km	0.031	1.22

Dramatic reduction of joint detections without LF in both cases!

Conclusions

- All the triangular and 2L geometries that have been investigated can be the baseline of a **superb 3G detector**, that will allow to improve by orders of magnitude compared to 2G detectors
- The **2L-15km-45° configuration** in general offer a better scientific return with respect to the Δ -10km, and has a similar performance on all parameters (for both BBHs and BNSs) to the **Δ -15km**
- The **low frequency sensitivity** is crucial for exploiting the full potential of ET. In the HF-configuration only, independently of the chosen geometry, several scientific targets would be lost or significantly diminished
- **Data analysis** for the next-generation poses a great **challenge**

Thank You!



ulyana.dupletsa@gssi.it

